Protic Conversion of Nitrile into Azavinylidene Complexes of Rhenium, a Mechanistic Theoretical Study

Maxim L. Kuznetsov,[†] Alexey A. Nazarov,[‡] and Armando J. L. Pombeiro*,[†]

Centro de Química Estrutural, Complexo I, Instituto Superior Técnico, Av. Rovisco Pais, 1049-001 Lisbon, Portugal, and Institute of Inorganic Chemistry—Bioinorganic, Environmental and Radiochemistry, University of Vienna, Waehringerstrasse 42, A-1090, Vienna, Austria

Received: May 26, 2005; In Final Form: July 21, 2005

The mechanism of the protonation of the rhenium nitrile chloro-complexes $[ReCl(NCCH_3)(PH_3)_4]$ (**2**), taken as models of the real systems $[ReCl(NCR)(dppe)_2]$ (dppe = $Ph_2PCH_2CH_2PPh_2$), leading to the azavinylidene products $[ReCl(NC(H)CH_3)(PH_3)_4]^+$ (**3**) was investigated by theoretical methods at the B3LYP level of theory. Electrostatic and molecular orbital arguments and thermodynamic, kinetic, and steric factors are analyzed and indicate that the chlorine atom is the most probable site of the initial proton attack, although the direct protonation of the nitrile carbon atom is also possible as a concurrent process. For the cis-isomer of **2**, the initially formed chloro-protonated species *cis*-$[Re(ClH)(NCCH_3)(PH_3)_4]^+$ further converts to the azavinylidene ***cis*-3** via either an acid-independent 1,4-proton shift or an acid−base catalyzed pathway involving a second protonation of the nitrile carbon atom to give *cis*-$[Re(ClH)(NC(H)CH_3)(PH_3)_4]^{2+}$ followed by elimination of the proton from the chlorine atom.

Introduction

Organonitriles (N≡CR) represent an important class of compounds that can form complexes with a variety of transition metals. The interest in the reactivity of nitriles at metal centers is accounted for by the possibility to use *coordinated* N≡CR as synthons for the preparation of compounds with newly created CC, CN, CO, CP, and CS bonds which cannot be easily synthesized without the involvement of a transition metal.[1−5] Among them, compounds such as tetrazoles, oxadiazoles, oxadiazolines, iminoesters, and different amides (e.g. nicotineamide and acrylamide), with pharmacological and industrial significance, can be mentioned.

Uncoordinated nitriles are commonly inert in chemical processes and react, as a rule, under harsh conditions with low yields of products. On the contrary, the reactivity of nitriles bound to suitable transition metal centers can dramatically increase, demonstrating the well-known activation of NCR by a metal. There are three main types of nitrile activation:[1−5] (i) toward nucleophilic addition at the nitrile C atom (Scheme 1A), (ii) toward electrophilic attack to the same carbon atom (Scheme 1B), and (iii) toward cycloaddition to the C≡N triple bond (Scheme 1C). Variation of a transition metal center can allow the switch of these reactivity modes. Hence, usage of transition metals in high oxidation states facilitates the nucleophilic addition due to shifting of the electron density from the ligand to the metal, what makes the β-carbon atom more positively charged. In contrast, an electron-rich metal center, with the metal in a low oxidation state and with a strong π-electron release ability, can activate a ligated nitrile to an electrophilic addition.

The first and third types of nitrile reactions have been studied intensively by us and others. They include the additions of a variety of nucleophiles such as water,[6a,b] alcohols,[6c,d] amines,[6e] sulfimides,[7] oximes,[8] hydroxylamines,[9] and hydroxamic acids[10] and the cycloadditions of various dipoles such as azides,[11] nitrones,[12] and nitrile oxides[13] to nitriles ligated to transition metals.

SCHEME 1: Types of Activation of Nitriles

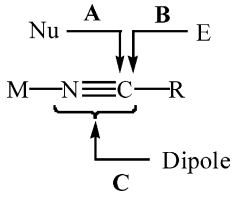

However, the second type of nitrile reactivity, i.e., the electrophilic addition reactions at a η^1-ligated nitrile, has only been scarcely explored.[1,5,14] Proton is the simplest electrophile and the protonation reactions of nitriles, in the η^1-mode, have so far been achieved at electron-rich d^6 Re,[15−19] Mo, or W[20−24] centers that can also bind dinitrogen which, at the latter sites, is activated toward protonation[25−27] to yield hydrazine or ammonia via hydrazido [M]−NNH_x (x = 1, 2) species which have been proposed to be key intermediates in the nitrogenase reduction of N_2 to NH_3 (Scheme 2A).

Nitriles are alternative substrates of nitrogenase, being reduced to amines, ammonia, and alkanes, and their enzymaic reduction has also been postulated[4,28] to occur via protonated intermediates in particular the azavinylidene (or methyleneamide) [M]−N=C(H)R species formed upon the first proton addition (Scheme 2B). This type of compound was first obtained by one of us by protonation of the rhenium nitrile chloro complexes *trans*-/*cis*-$[ReCl(NCR)(dppe)_2]$ (**1**, dppe = $Ph_2PCH_2CH_2PPh_2$),[15,18,19] which affords the corresponding azavinylidene products $[ReCl(NC(H)R)(dppe)_2]^+$.

Stopped-flow kinetic investigations indicated that the general rate law for the protonation of **1** includes two terms—an acid-

* To whom correspondence should be addressed. Fax: +351-21-846-4455. E-mail: pombeiro@ist.utl.pt.
† Instituto Superior Técnico.
‡ University of Vienna.

10.1021/jp0527913 CCC: $30.25
Published on Web 08/20/2005

SCHEME 2: Postulated Initial Protonation Reactions in the Nitrogenase Reduction of Dinitrogen (A) and Organonitriles (B)

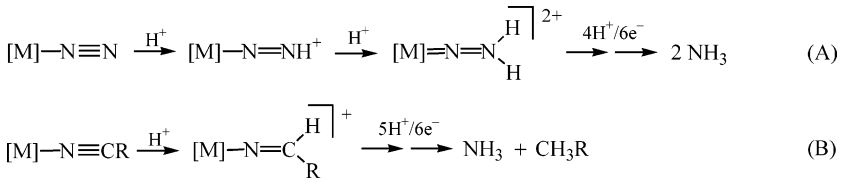

SCHEME 3: Corrected Mechanism of Protonation of the Nitrile Complexes *trans*-/*cis*-[ReCl(NCR)(dppe)$_2$] (See Text)

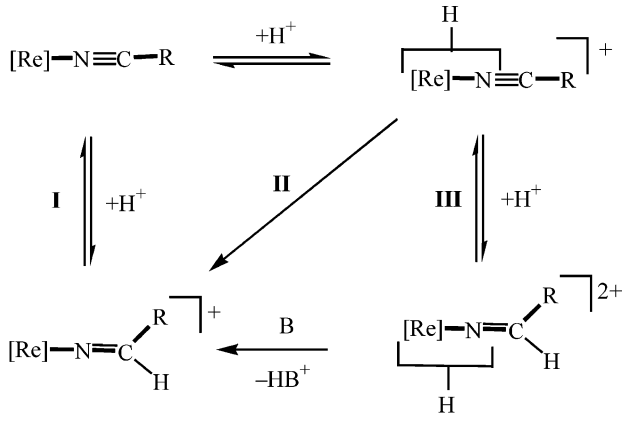

[Re] = *trans*-/*cis*-{ReCl(dppe)$_2$}

B = base (solvent, Cl^- or HCl)

independent one and an acid-dependent one. However, the initially proposed[18] mechanistic scheme for this reaction needs to be amended since the protonation products first formulated as the hydrides $[ReCl(H)(NCR)(dppe)_2]^+$ were later unambiguously shown[19] to be the trans-isomers of the azavinylidene complexes, i.e., the proton added to the nitrile rather than to the metal. The corrected form is now given in Scheme 3, which shows that the protonation of the nitrile complex **1** occurs via three competitive pathways. One of them (**I**) consists on the direct protonation at the nitrile carbon atom, whereas the others involve the initial protonation of another site of the molecule and then either an intramolecular proton migration to the C atom (acid-independent route, **II**) or a second protonation at the C atom, followed by the first proton elimination (acid−base catalyzed route, **III**). The intermediate formed upon the initial protonation was neither identified nor detected due to its short lifetime. Hence, some mechanistic features of this reaction still remain elusive, but theoretical methods are expected to provide an alternative approach toward their elucidation.

Thus, the main goal of the present work − which is a continuation of our experimental[6a,b,7−10,12b−d,13b,15,17−19] and theoretical[6b,c,7,8a,d,10,12a,13a,29] studies in the field of reactivity of organonitrile ligands − is to identify the plausible mechanisms of the protonation of the complexes *trans*-/*cis*-$[ReCl(NCCH_3)(PH_3)_4]$ (**2**) taken as a models of the real systems **1**, including the determination of the most probable site of the initial protonation and further steps of the proton migration. The article has the following structure. First, the initial site of the proton attack is discussed in terms of electrostatic and frontier-molecular orbitals arguments and the HSAB principle, and second, the acid-independent, the acid−base catalyzed, and the combined pathways of the following conversions to the final azavinylidene product are described.

Computational Details

The full geometry optimization of all structures and transition states has been carried out at the DFT level of theory using a quasi-relativistic effective core potentials (ECPs)[30] with the help of the Gaussian-98[31] program package. The calculations have been performed using Becke's three-parameter hybrid exchange functional[32] in combination with the gradient-corrected correlation functional of Lee, Yang, and Parr[33] (B3LYP). This functional was found to be a quite reasonable one for the investigation of the reactivity, electrochemical behavior, structural and spectral properties, and bonding of rhenium and platinum nitrile complexes, taking into account the low computational cost of this method and the fact that the results obtained at B3LYP often well agree with the experimental ones and with those calculated at the higher correlated methods.[12a,29]

A quasi-relativistic Stuttgart pseudopotential described 60 core electrons and the appropriate contracted basis set (8s7p6d)/[6s5p3d][34] for the rhenium atom and the 6-31G* basis set for other atoms were used. To investigate the influence of the basis set on the relative energies, some key structures have been optimized using the B3LYP/6-31+G* level for the nonmetal atoms with following single-point calculations at B3LYP/6-311++G**. Such improvement of the basis set affects the activation parameters and reaction energies rather weakly (by 0.0−3.8 kcal/mol; see the respective tables) and does not change the main conclusions of the present work.

Symmetry operations were not applied for all structures. The Hessian matrix was calculated analytically for all optimized structures in order to prove the location of correct minima (no "imaginary frequencies") or saddle points (only one negative eigenvalue) and, to estimate the zero-point energy correction and thermodynamic parameters, the latter were calculated at 25 °C. The nature of the transition states was investigated by the analysis of the vectors associated with the "imaginary frequency" and, in some cases, by the intrinsic reaction coordinate (IRC) calculations.[35]

Solvent effects were taken into account at the single-point calculations on the basis of the gas-phase geometries using the polarizable continuum model[36] in the CPCM version[37] with CH_2Cl_2 as a solvent. The free Gibbs energies in the solution (G_s) were estimated by addition of the ZPE, thermal and entropic contributions taken from the gas-phase calculations (δG_g) to the single-point CPCM-SCF energy (E_s).

The electrostatic potential (ESP) values were determined for the grid of points in the plane containing the Re, N, and Cl atoms (for the cis-isomers) or the Re, N, and one of P atoms (for the trans-isomers) and in the parallel planes (at distances of 1 and 2 Å from the former plane). For the monoprotonated structures, the ESP calculations have been performed also in the planes perpendicular to those defined above.

For the HSAB consideration, the global softness (S) was calculated as[38]

$$S \approx 1/(I - A)$$

where I and A are the vertical ionization potential and electron affinity, respectively. Fukui functions of the atom x in a molecule with N electrons, f_x^+ and f_x^- (the former for nucleophilic attack and the latter for electrophilic attack) were defined in a finite-difference approximation using the equations[39]

$$f_x^+ = [q_x(N+1) - q_x(N)]$$

$$f_x^- = [q_x(N) - q_x(N-1)]$$

where q_x is the NBO[40] electronic population of atom x in a molecule. The local atomic softnesses s_x^+ and s_x^- were calculated as

$$s_x^+ = f_x^+ S \quad \text{and} \quad s_x^- = f_x^- S$$

The hypothetical complexes *trans*-/*cis*-[ReCl(NCCH$_3$)(PH$_3$)$_4$] (**2**) with four phosphine ligands instead of the real ones *trans*-/*cis*-[ReCl(NCR)(dppe)$_2$] (**1**) (R = alkyl or aryl, dppe = Ph$_2$PCH$_2$CH$_2$PPh$_2$) were chosen as model compounds for our calculations. The validity of such a simplification, i.e., the consideration of a pair of monodentate PH_3 phosphines instead of each bidentate phosphine ligand, was proved previously.[41]

Results and Discussion

Reactions of electrophilic addition, in general, and of protonation, in particular, have been *theoretically* investigated in a number of cases, usually involving free nucleophiles. They include halogenation of olefins, alkynes, and allenes,[42] reaction of S_2^{2+} with alkenes,[43] protonation of olefins,[44] alkanes,[45] ketenes,[46] thiouracils,[47] chlorine nitrate,[48] phenanthrolines,[49] macrocycles,[50] quinolines, benzazepines, and acetanilides,[51] boranes,[52] and thiazoles,[53] and anti-Mills−Nixon systems.[54] Less studied is the electrophilic addition to a substrate activated upon coordination, examples including interaction of weak acids and aldehydes with bis-allylpalladium complexes,[55] addition of CO_2 to 2-lithio-1,3-dithiane,[56] addition of methyl cation to arene tricarbonylchromium complexes,[57] and protonation of η^2-allene,[58] of η^2-alkynes,[59] of biological macromolecules,[60] and of titanium peroxo complexes.[61] Moreover, the electrophilic addition to nitriles, either free or coordinated to a transition metal, has not yet been studied theoretically and this work, to the best of our knowledge, is the first attempt to fill this gap.

1. Initial Site of the Proton Attack. The first step of the investigation of the mechanism concerns the geometry optimization of the starting complexes *trans*-/*cis*-[ReCl(NCCH$_3$)(PH$_3$)$_4$] (***trans*-2**/***cis*-2**) and of the possible protonated structures and the analysis of the factors determining the most plausible site of the protonation. The equilibrium structures of **2** (Figure 1) have been discussed previously,[29] and, within the current work, we reoptimized them at the more extended basis set. The structural parameters obtained at B3LYP/6-31G* are given for comparison in Table 1 and Table 1S (Supporting Information) and are reasonably consistent with those calculated at the other levels previously used. Improving the basis set resulted in a better agreement of the theoretical structural parameters of ***trans*-2** with the experimental ones for the complex *trans*-[ReCl(NCCH$_3$)(dppe)$_2$].[62] The maximum deviation of 0.04 Å was found for the Re−Cl and Re−N bonds.

Charge Control Considerations. The reactivity of complexes **2** toward the electrophilic addition can be interpreted in terms of charge control arguments. Let us first examine the effective atomic charge distribution in the starting nitrile complexes. The charges have been calculated using both Mulliken and NBO partitioning schemes. The results, presented in Table 2, demonstrate a disagreement between these two methods. For the Mulliken scheme, the most negative charge is localized at the γ-C and N atoms (−0.51 and −0.41) whereas less negative values were obtained for the Cl and Re atoms. However, the charge distribution is opposite for the NBO method, i.e., the Re atom is the most negatively charged one (−0.93 to −0.97) being followed by the γ-C, Cl and N atoms (−0.77, −0.55, −0.32). Such inconsistency prevents any plausible conclusion about the most probable site of the proton attack. It is noteworthy to indicate that the consideration of the solvent effects does not result in any significant changes of the atomic charges.

To clarify the situation and to determine the most probable ways of H^+ approaching, calculations of the electrostatic potential (ESP) distribution have been performed and the results are illustrated (Figure 2) by the maps of negative ESP for the plane containing the Re, N, C, Cl, and two P atoms (z = 0 Å) and for the parallel plane at 1 Å distance (z = 1 Å). The most extended region of the negative ESP is located near the Cl atom (I, Figure 2) with the maximum potential value of ca. −0.09 au. Meanwhile, the borderline of this region, in some parts, is situated rather close to the Re atom at the distance of 1.5 Å, and, for the cis-isomer, to the N and C atoms. Besides, a couple of less extended regions with smaller negative ESP values are placed near the Re, N, and C atoms (II and III, Figure 2). The consideration of the solvent effects does not affect significantly the general view of the ESP distribution and the values of the potential. Thus, a simple examination of the ESP distribution suggests that the easiest way for proton attack is to the chlorine atom taking into account the closeness of the extended region with the most negative ESP, the comparatively high effective atomic charge and the absence of steric hindrances during H^+ approaching. This result is coherent with that obtained previously for the protonation of the allene rhenium complex *trans*-[ReCl(η^2-H$_2$C=C=CH$_2$)(PH$_3$)$_4$].[58] Meanwhile, the Re, N, and β-C atoms cannot be excluded at this stage as possible, although less probable sites of protonation.

On the next step of the calculations, the geometry optimization of eventual protonated structures has been carried out. The calculations were performed for the initial proton position in the regions with the negative ESP (see Figure 2). The minima on the potential energy surface were found for all the following monoprotonated structures (the total energies, enthalpies and free Gibbs energies of all calculated structures are given in Table 2S, Supporting Information). The most stable ones are those with the protonated β-C atom (**3**+, Figure 1), presenting the final product of the reaction. These structures are formed when the proton approaches from points 1 and 2 (Figure 2A) and points 1−3 (Figure 2B), demonstrating the possibility of the direct protonation of this atom. For the cis-isomer, two structures, ***cis*-3a**+ and ***cis*-3b**+, with different conformations of the NC(H)CH$_3$ fragment and very close energies were found.

The structural parameters of ***trans*-3**+ (Tables 1 and 1S) are in good agreement with the X-ray structural data for the complex *trans*-[ReCl{NC(H)C$_6$H$_4$F-4}(dppe)$_2$][BF$_4$][19] with the maximum deviation of 0.066 Å for the Re−Cl bond and not higher than 0.025 Å for the other bonds. All complexes **3**+ correspond to the linear coordination mode of the azavinylidene ligand with the ReNC angle of 179° that allows the description of NC(H)CH$_3$ as a three-electron donor **a**, conferring the 18-electron configuration to the complex. The Re−N distance (1.844−1.857 Å) is consistent with a significant double character of this bond being by 0.174−0.217 Å shorter than that calculated for **2**. The

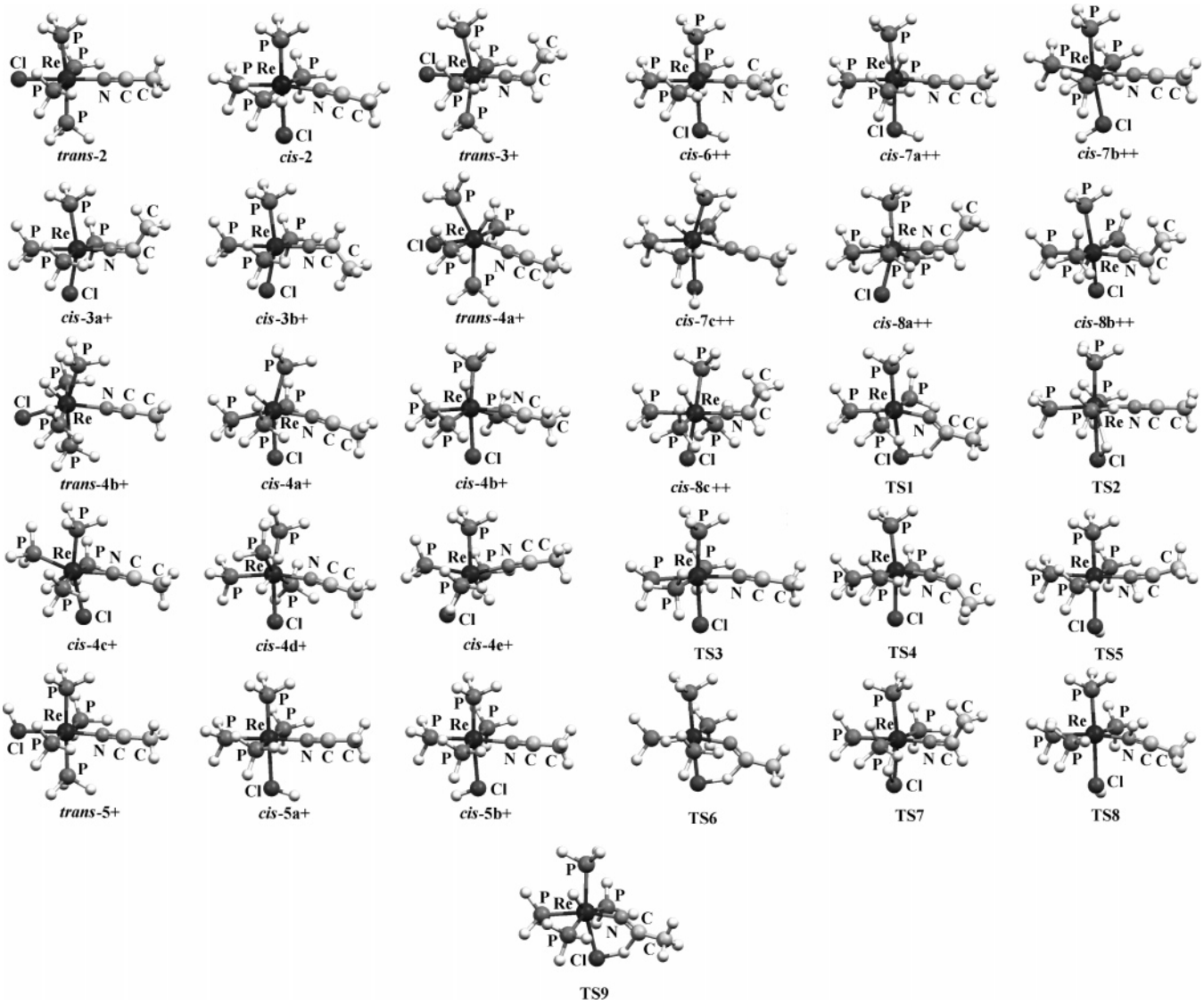

Figure 1. Equilibrium geometries of calculated structures and transition states.

Re−Cl bond of **3**+ is also significantly shorter than that in **2** while the Re−P bond becomes longer, in accord with the increase of the oxidation state of the metal which thus becomes a better electron-acceptor from the Cl ligand and a poorer π-electron releaser to the phosphines. The ligand NC bond stretches, as expected. It is worthwhile to mention that the extensive search of the potential energy surface (PES) for the C-monoprotonated complexes did not result in the location of a minimum for the 16-electron bent structure **b**, since geometry optimization led only to the linear ReNC fragment.

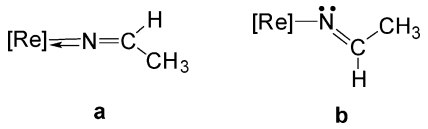

a **b**

The second most stable structures (**4**+, Figure 1) are those with the protonated rhenium atom (five for the cis- and two for the trans-isomer). For the trans-geometry, both complexes (***trans*-4a**+, ***trans*-4b**+) have pentagonal bipyramidal structures and are formed upon H^+ approaching from the points 3−7 (Figure 2A). For the cis-isomers, three pentagonal bipyramidal structures (***cis*-4b**+, ***cis*-4d**+, and ***cis*-4e**+, H^+ starting from points 4−7, Figure 2B) and two others with coordination polyhedra between a bipyramid and a capped octahedron (***cis*-4a**+ and ***cis*-4c**+, H^+ starting from points 8−10, Figure 2B) were obtained. The hydride complexes have shortened Re−Cl bonds in comparison with the parent **2**, whereas the Re−P and Re−N bonds become longer, consistent with the increase of electron-acceptor ability of the metal and the decrease of its π-electron releasing character, upon oxidation, to the phosphines and nitrile ligands.

Finally, three other less stable structures (**5**+, Figure 1) with the protonated Cl atom were found. The ***cis*-5a**+ and ***cis*-5b**+ species differ in the position of the Cl−H bond relative to the rest of the molecule, and a simple interconversion between these structures is expected due to the easy rotation around the Re−Cl bond. The complexes **5**+ are formed when the proton approaches the molecule from the side of the ligating chloride, i.e., from the extended region with the most negative ESP values. The protonation of the Cl atom results in only moderate structural changes and affects mainly the Re−Cl bond whose length increases to 2.641−2.687 Å indicating a pronounced weakening of this bond. No structures with the protonated N atom have been located even when the H^+ was placed near the nitrogen at the distance of 1 Å.

Orbital Control Considerations. Another driving force for the reaction concerns the interaction of the valence MOs of the

TABLE 1: Selected Bond Lengths (Å) of the Key Calculated Structures[a]

	***trans*-2**[b]	***cis*-2**	***trans*-3+**[c]	***trans*-4a+**	***trans*-5+**
Re−Cl	2.575 [2.531(2)]	2.555	2.503 [2.437]	2.524	2.641
Re−$P_{trans-to-Cl}$		2.319			
Re−$P_{trans-to-N}$		2.367			
Re−P	2.378 [2.374(2)−2.420(2)]	2.381, 2.382	2.425−2.471 [2.436−2.487]	2.409,2.506	2.399, 2.408
Re−N	2.018 [1.978(5)]	2.074	1.844 [1.831]	2.098	2.027
C≡N	1.171 [1.141(9)]	1.163	1.269 [1.244]	1.159	1.165
C−C	1.460 [1.480(11)]	1.459	1.508	1.458	1.460
Re−H/Cl−H				1.672	1.300

	***cis*-3b+**	***cis*-4a+**	***cis*-4d+**	***cis*-5a+**	***cis*-6++**
Re−Cl	2.433	2.515	2.509	2.669	2.691
Re−$P_{trans-to-Cl}$	2.430	2.390	2.429	2.325	2.366
Re−$P_{trans-to-N}$	2.570	2.135	2.383	2.386	2.588
Re−P	2.425	2.426, 2.436	2.398, 2.501	2.401	2.487, 2.491
Re−N	1.857	2.135	2.121	2.093	1.855
C≡N	1.263	1.159	1.160	1.164	1.266
C−C	1.508	1.457	1.458	1.460	1.506
Re−H/Cl−H		1.669	1.682	1.298	1.301

	***cis*-7a++**	***cis*-8c++**	**TS1**	**TS2**
Re−Cl	2.680	2.429	2.568	2.838
Re−$P_{trans-to-Cl}$	2.395	2.495	2.375	2.317
Re−$P_{trans-to-N}$	2.438	2.568	2.449	2.387
Re−P	2.457, 2.505	2.482, 2.542	2.414, 2.415	2.405, 2.413
Re−N	2.134	1.881	1.976	2.100
C≡N	1.161	1.259	1.205	1.163
C−C	1.458	1.507	1.482	1.459
Re−H	1.655	1.677		2.332
Cl−H	1.300			1.325

[a] Experimental values for some of the real complexes are also given for comparison. [b] For *trans*-[$ReCl(NCCH_3)(dppe)_2$] in square brackets. [c] For *trans*-[$ReCl\{NC(H)C_6H_4F\text{-}4\}(dppe)_2][BF_4$] in square brackets.

TABLE 2: NBO and Mulliken (in Parentheses) Atomic Charges for the Initial and Selected Monoprotonated Structures

atom	***trans*-2**	***cis*-2**	***trans*-3+**	***cis*-3b+**	***trans*-4a+**	***cis*-4a+**
Re	−0.93 (−0.25)	−0.97 (−0.39)	−0.39 (−0.25)	−0.39 (−0.30)	−0.78 (−0.55)	−0.82 (−0.61)
Cl	−0.55 (−0.32)	−0.55 (−0.34)	−0.44 (−0.19)	−0.35 (−0.20)	−0.39 (−0.34)	−0.43 (−0.22)
P	0.35 (0.07)	0.34−0.35 (0.05−0.13)	0.30−0.31 (0.14−0.16)	0.22−0.31 (0.13−0.17)	0.31−0.41 (0.32−0.43)	0.31−0.40 (0.14−0.24)
N	−0.32 (−0.42)	−0.32 (−0.41)	−0.32 (−0.42)	−0.34 (−0.42)	−0.35 (−0.56)	−0.39 (−0.45)
C	0.32 (0.27)	0.39 (0.31)	0.02 (0.01)	0.06 (0.03)	0.47 (0.38)	0.50 (0.38)
C	−0.77 (−0.51)	−0.78 (−0.51)	−0.72 (−0.51)	−0.73 (−0.52)	−0.80 (−0.55)	−0.80 (−0.52)

atom	***cis*-4d++**	***trans*−5+**	***cis*−5a+**
Re	−0.81 (−0.54)	−0.94 (−0.30)	−0.98 (−0.44)
Cl	−0.37 (−0.20)	−0.10 (−0.05)	−0.11 (−0.05)
P	0.31−0.41 (0.09−0.22)	0.30 (0.07−0.09)	0.30−0.40 (0.10−0.14)
N	−0.38 (−0.43)	−0.32 (−0.43)	−0.38 (−0.45)
C	0.47 (0.38)	0.40 (0.31)	0.43 (0.34)
C	−0.79 (−0.52)	−0.79 (−0.52)	−0.79 (−0.52)

reactants. From frontier molecular orbitals (FMO) theory[63] viewpoints, the electrophilic attack, e.g., protonation, should be determined by the composition and energy of the HOMO of the complex. The composition of FMOs of **2** has been described previously in detail.[29] The HOMO is mainly centered on the metal atom but also includes p-orbitals of the Cl and β-C atoms with noticeable contributions (Figure 3). Therefore, any of these three atoms, but especially Re, are favorable for protonation in terms of frontier-orbital arguments.

HSAB Considerations. One of the useful tools for the determination of the most plausible site of an electrophilic or nucleophilic attack is the "hard−soft acid−base" (HSAB) principle[38] initially based on the global reactivity descriptors, i.e., hardness (η) and softness (S), determining the chemical behavior of the molecule as a whole. Reactivity of a particular site of the molecule can be described in terms of the local properties, first of all, such as Fukui functions (f) and local softness (s), which were used successfully to make predictions for various types of the nucleophilic additions, electrophilic additions, and cycloadditions.[64−66] As was shown recently,[66] the ratios s^+/s^- and s^-/s^+, called "relative electrophilicity" and "relative nucleophilicity", respectively, reproduce experimental trends better than the individual s^+ and s^- values. The site of the molecule with the highest s^+/s^- value is, thus, the most susceptible to the nucleophilic attack and the site with the highest s^-/s^+ parameter is the most probable for the electrophilic attack.

The calculated vertical values of ionization potential (I) and electron affinity (A) and the global softness (S), for ***trans*-2** and ***cis*-2**, as well as the local properties (f^+, f^-, s^+, s^-, s^-/s^+), for three possible centers of protonation, are given in Table 3. As it can be seen, the maximum values of both s^+ and s^- individual local softnesses are highest for the metal atom. However, the

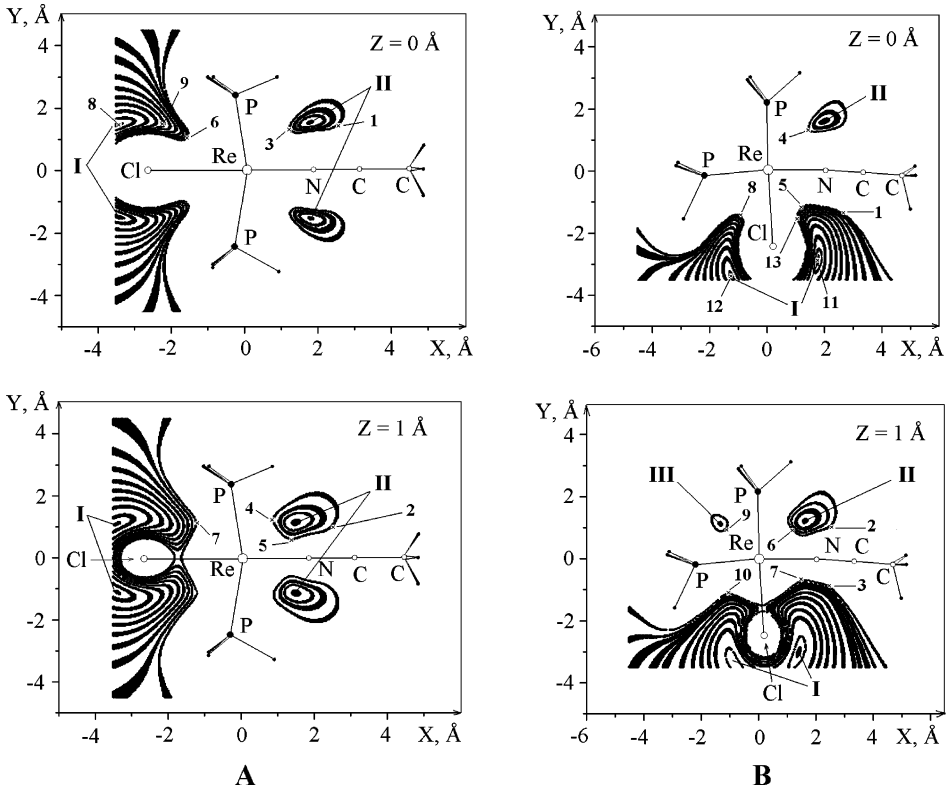

Figure 2. Distribution of negative electrostatic potential for the complexes ***trans*-2** (A) and ***cis*-2** (B). The points with maximum values of negative ESP are indicated by Roman numerals, the points of the initial proton position at the geometry optimization of the monoprotonated structures are indicated by Arabic numerals.

relative nucleophilicity s^-/s^+ is highest for the chlorine atom followed by the β-carbon (for ***cis*-2**) and rhenium atoms indicating that the halide is the most probable site of protonation.

The results presented above, considered altogether, suggest that, although any of the three Cl, β-C and Re atoms can be protonated without overcoming of a potential barrier, the chloro-atom is the most probable site of proton attack (to give **5**+) because (i) the Cl atom has a strong negative atomic charge and it is surrounded by the extended region with the most negative ESP; (ii) the proton approach to Cl is not hampered by any steric hindrance; (iii) there is a significant contribution of *p*(Cl) orbitals to the HOMO of **2** (although lower than that of the metal); (iv) the highest value of the relative nucleophilicity s^-/s^+ lies on the Cl atom; (v) in comparison with other monoprotonated structures, the formation of the complexes with protonated Cl ligand (**5**+) requires the smallest structural changes relative to the parent nitrile species **2** (this is in agreement with the experimental data that show an initial fast protonation step, occurring quantitatively during the short deadtime, 2 ms, of the stopped-flow spectrophotometer).

The direct protonation of the β-C atom to give the final product **3**+ is also possible from both charge and orbital control viewpoints. This route is more thermodynamically favored than that of the protonation of the chlorine atom (due to the higher stability of **3**+ than **5**+) but less favored in terms of electrostatic arguments (positive atomic charge on the C atom and much less extended regions with negative ESP in comparison with Cl) and HSAB considerations. Thus, these routes can be competitive, in accord with the experimental data.[18,19]

The initial formation of the hydride species—the intermediate postulated earlier[18]—could not be ruled out, in principle, due to the great involvement of the *d*(Re) orbitals in the HOMO of **2** and the presence of regions with negative ESP near the Re atom. Nevertheless, the latter have a relatively small extension (regions II and III) and the proton placed at point 13 of the region I (Figure 2B) moves to the Cl rather than the Re atom at the geometry optimization. Taking also into account that the proton approach to rhenium is hampered sterically (especially for the real complexes containing bulky dppe ligands) and the formation of **4**+ (Re protonated structures) is accompanied by significant structural changes, such a route seems to be much less probable. In this respect, we should mention that we never obtained, in our extensive experimental protonation studies of [ReCl(L)-(dppe)$_2$] (L = CNR, NCR, alkyne, or any derivative), any hydride complex. Finally, the conversion of the rhenium-protonated species to the final azavinylidene complex cannot proceed easily (for the acid-independent pathway) in contrast to the case of the chloro-protonated intermediate (see below).

2. Acid-Independent Pathway. In view of the higher stability of ***cis*-1** in comparison with ***trans*-1**, the former complex was mainly investigated experimentally. Hence, the further steps of the protonation of **2** (as a model) were theoretically studied only for the *cis*-isomer. Taking into account the lowest stability of the chloro-protonated structures (**5**$^+$)—which are those most probably formed on the first stage—and the highest stability of the final C-protonated complexes (**3**$^+$), the **5**+ → **3**+ transformation (Scheme 4) is expected to occur on the next step of the reaction as a result of an intramolecular proton migration. This acid-independent pathway is discussed in this section, in terms of a single or a multistep process.

One-Step Route. For one-step proton migration from the Cl to the β-C atom, the five-membered cyclic transition state (**TS1**, Figure 1), with the proton situated between those atoms, has been located. The electronic activation energy in CH_2Cl_2 solution ($\Delta E_s^{\ddagger}$) for this process is rather low (15.17 kcal/mol, Table 4) providing an easy step for the reaction. The Gibbs free energy of activation in solution ($\Delta G_s^{\ddagger}$) is only by 1.02 kcal/

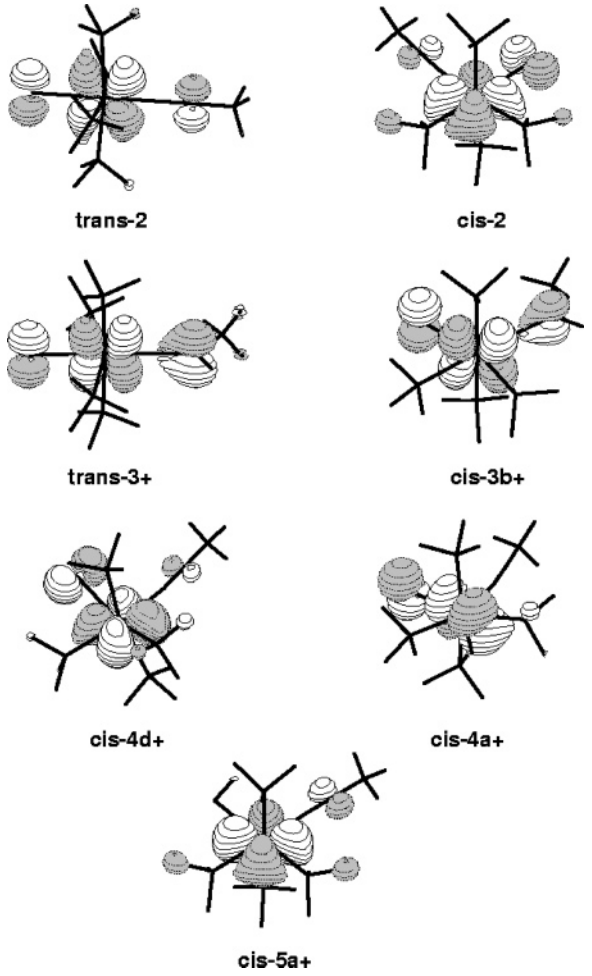

Figure 3. Plots of the HOMOs of **2** and some of the monoprotonated structures (contour values of 0.05).

mol lower than $\Delta E_s^{\ddagger}$ due to the small change of the entropy term ($\Delta S^{\ddagger} = -4.61$ cal/mol·K).[67]

Multistep Route. Besides the one-step pathway, the proton migration may occur in a multistep manner, i.e., via several 1,2- and/or 1,3-proton shifts. The most obvious and simple way is via the metal atom, i.e., through the consecutive **5**+ → **4**+ → **3**+ transformations. For the first step, i.e., the 1,2-H shift from Cl to the Re atom, a saddle point corresponding to the transition state (**TS2**) was found. Analysis of the nature of this TS suggests that the hydride complex ***cis*-4d**+ is formed from ***cis*-5a**+ as a result of such transformation (Scheme 4) with a low activation barrier ($\Delta G_s^{\ddagger} = 6.32$ kcal/mol, Table 4). No transition state leading to the ***cis*-4c**+ or ***cis*-4e**+ species was located.

However, the calculations indicate that the further direct ***cis*-4d**+ → ***cis*-3a**+ process does not occur. Indeed, all attempts to find the corresponding transition state led either back to **TS2** or to **TS1**, ***cis*-3a**+ or ***cis*-4d**+. Instead of this process, the more complicated ***cis*-4d**+ → ***cis*-4b**+ → ***cis*-3b**+ route was found to be realistic, in principle (Scheme 4). The first step, i.e., conversion between two hydride structures, proceeds via the transition state **TS3** with the proton between PH_3 and $NCCH_3$ ligands and with a pentagonal bipyramidal structure.[68] The activation barrier is rather low with the $\Delta G_s^{\ddagger}$ value of 5.37 kcal/mol.

The final step, involving the 1,3-H-shift ***cis*-4b**+ → ***cis*-3b**+, proceeds via the transition state **TS4**. The hydrogen atom in **TS4** is situated near the N atom with the N···H and C···H distances of 1.147 and 1.439 Å. However, the activation barrier found for this transformation is very high ($\Delta G_s^{\ddagger} = 62.84$ kcal/mol) what rules out such a multistep route and suggests that, within the acid-independent pathway, the reaction proceeds via one-step 1,4-proton migration.

3. Acid—Base Catalyzed Pathway. Following the initial protonation at the Cl ligand, the reaction may proceed (Schemes 3 and 4) via an acid−base catalyzed pathway, involving a second proton addition to the β-C atom to give ***cis*-6**++ and then elimination of the first proton (route 1). First, the possibility of the second protonation of the ***cis*-5a**+ protonated-chloro complex was investigated (Scheme 4).

$$\textit{cis}\text{-}\mathbf{5}+ \rightarrow \textit{cis}\text{-}\mathbf{6}++ \rightarrow \textit{cis}\text{-}\mathbf{3}+ \qquad (1)$$

Inspection of the effective atomic charges in ***cis*-5a**+ indicates that the Re atom has a strong negative charge (−0.98 for NBO) and, hence, it is still an attractive center for the second protonation. Similarly to the initial complex ***cis*-2**, for the ***cis*-5a**+ species the calculations of the ESP distribution have been performed (Figure 4A). As a result, no regions with negative ESP were found. However, the distribution of the positive ESP has a "channel" with the least positive values that would allow the comparatively easy penetration of the proton close to the C and Re atoms (see arrow on the Figure 4A). Moreover, the HOMO of ***cis*-5a**+ is formed by noticeable contributions of the orbitals of both Re and C atoms (Figure 3). However, the geometry optimization of the doubly protonated structure with the initial position of the second H^+ in the "orifice" of the channel (point 1, Figure 4A) resulted in the formation of the complex ***cis*-6**++ with the second proton at the β-C atom, and only the deeper initial position of the proton, at point 2, led to the hydride complex ***cis*-7a**++. The formation of the latter structure is by 2.57 kcal/mol less energetically favored than that of the former one (Table 4).[69]

The structural changes upon the ***cis*-5a**+ → ***cis*-6**++ reaction are similar to those for the ***cis*-3**+ → ***cis*-2** transformation, which also involves protonation of a nitrile ligand. The proton addition to the β-C atom also accounts for an increase of the acidity of the HCl ligand. Indeed, the deprotonation energy difference for the two processes, i.e., ***cis*-6**++ → ***cis*-3b**+ and ***cis*-5a**+ → ***cis*-2** [$\Delta\Delta G_s = (G_s^{cis-3b+} - G_s^{cis-6++}) - (G_s^{cis-2} - G_s^{cis-5a+})$] is −37.40 kcal/mol. Within the structure ***cis*-6**++, the HCl ligand exhibits also a higher acidity in comparison with the azavinylidene, the corresponding parameter $\Delta\Delta G_s = G_s^{cis-3b+} - G_s^{cis-5a+}$ being −19.02 kcal/mol. Thus, the reaction ***cis*-6**++ → ***cis*-3**+ should proceed easily, especially in the presence of any base such as Cl^-, the solvent (CH_2Cl_2) or even HCl (a weak

TABLE 3: Calculated Ionization Potentials (*I*), Electron Affinities (*A*), Fukui Functions (f^+, f^-), Global (S) and Local (s^+, s^-) Softnesses and Relative Nucleophilicity (s^-/s^+) in Atomic Units

	I		A		S
trans*-2**/cis*-2**	0.2136/0.2219		–0.0057/–0.0070		4.5600/4.3687
Atom	f^+	s^+	f^-	s^-	s^-/s^+
Cl	0.0175/0.0169	0.0798/0.0737	0.1749/0.1747	0.7975/0.7631	9.9937/10.3541
Re	0.7799/0.7861	3.5563/3.4341	0.4000/0.3908	1.8240/1.7071	0.5129/0.4971
β-C	–0.0046/0.0060	–0.0210/0.1147	0.1489/0.1129	0.6790/0.4932	—/4.3000

SCHEME 4: Plausible Mechanisms of *cis*-5a+ to *cis*-3+ Conversion

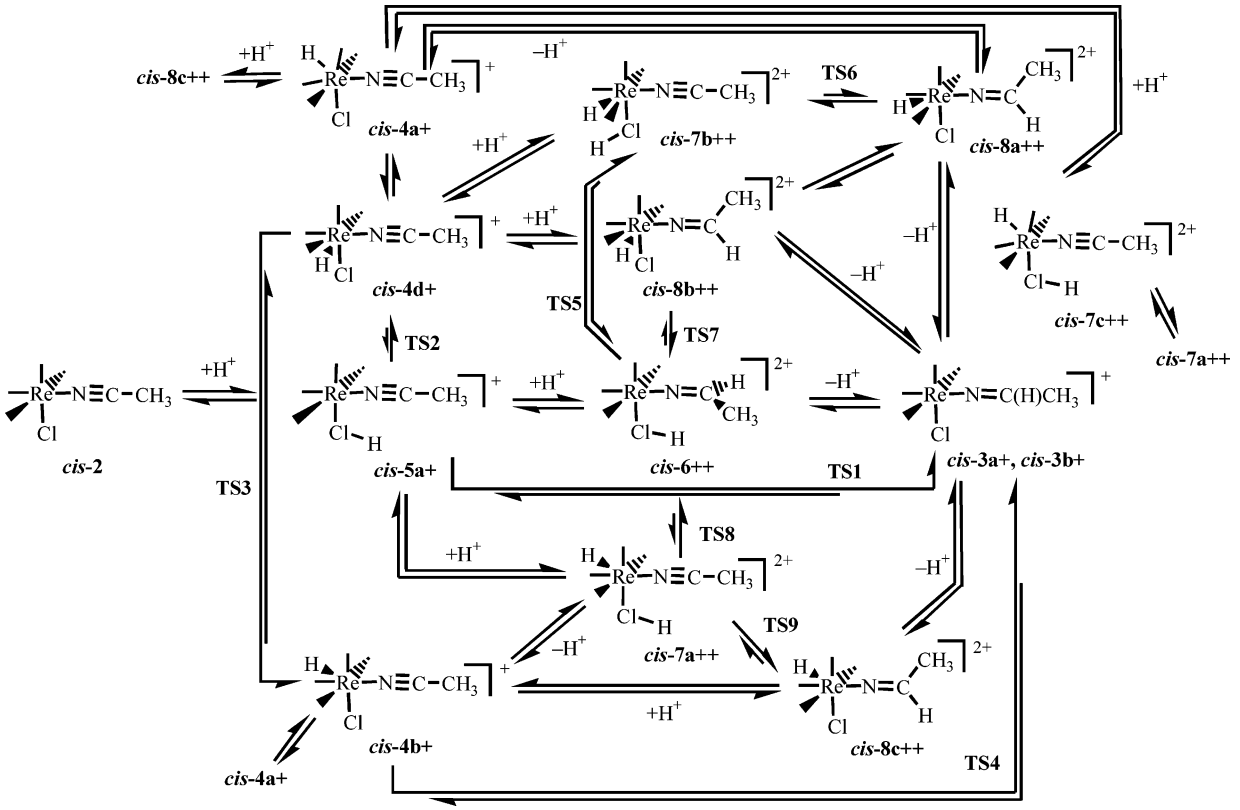

TABLE 4: Electronic Activation Energy, E_a, Enthalpy and Free Gibbs Energies of Activation, $\Delta H^{\ddagger}$ and $\Delta G^{\ddagger}$, and Reaction Energies, ΔE, ΔH, and ΔG (in kcal/mol) of the H-Migration Processes[a]

process	E_a	$\Delta H^{\ddagger}$	$\Delta G^{\ddagger}$	ΔE	ΔH	ΔG
***cis*-5a+ → TS1 → *cis*-3a+**	15.42	13.03	14.40	−20.41	−18.54	−16.14
	15.38[b]	13.00[b]	15.27[b]	−20.72[b]	−18.82[b]	−16.36[b]
	16.44[c]		**14.15**	−16.57[c]		**−18.35**
	15.17			**−22.62**		
***cis*-5a+ → TS2 → *cis*-4d+**	5.58	4.38	5.12	−4.23	−3.64	−1.35
	6.78		**6.32**	**−6.54**		**−3.66**
***cis*-4d+ → TS3 → *cis*-4b+**	6.54	5.83	6.20	−10.91	−10.86	−11.09
	5.71		**5.37**	**−9.79**		**−9.98**
***cis*-4b+ → TS4 → *cis*-3b+**	70.03	67.43	65.81	−6.03	−4.80	−4.48
	67.05		**62.84**	**−6.93**		**−5.39**
***cis*-7b++ → TS5 → *cis*-6++**	63.09	61.13	58.69	+0.43	+2.29	+0.58
	58.58		**54.18**	**−1.22**		**−1.07**
***cis*-7b++ → TS6 → *cis*-8a++**	28.91	26.90	27.81	+4.13	+6.15	+6.50
	26.98		**25.87**	**+0.28**		**+2.64**
***cis*−8b++ → TS7 → *cis*-6++**	7.37	5.02	4.17	−10.67	−10.88	−13.46
	9.67		**6.46**	**−7.98**		**−10.77**
***cis*−7a++ → TS8 → *cis*-6++**	61.75	59.76	57.76	−1.28	+0.53	−1.27
	57.42		**53.43**	−1.15[b]	+0.48[b]	−1.46[b]
				−0.31[c]		**−2.57**
				−2.57		
***cis*−7a++ → TS9 → *cis*-8c++**	25.35	23.42	24.45	−3.55	−1.34	−0.15
	24.12		**23.22**	−4.13[b]	−2.48[b]	−0.02[b]
				−0.66[c]		**−2.80**
				−6.20		

[a] Energies corrected on the solvent effect are given as a bold text. [b] Energies calculated at the B3LYP/6-31+G*//B3LYP/6-31+G* + ECP (Re) level. [c] Energies calculated at the B3LYP/6-311++G**//B3LYP/6-31+G* + ECP (Re) level.

acid in this solvent), thus completing the acid−base catalyzed pathway to afford the final azavinylidene complex ***cis*-3+**.

Although the formation of the complex ***cis*-7a++** is less probable than that of ***cis*-6++** (see above and also taking into account the higher steric hindrance and significant distortion of the coordination polyhedron upon Re protonation) and the direct conversion of ***cis*-7a++** to the final product in one step is impossible, combined pathways based on this structure cannot be completely ruled out and are discussed below.

4. Combined Pathways. Routes Based on the Hydride *cis*-4d+ Structure. The low activation barrier for the ***cis*-5a+ → *cis*-4d+** conversion (H^+ shift from the Cl to the Re atom) and the slightly higher stability of the latter (by 3.66 kcal/mol) suggest that these two species easily interconvert, and both the chloro-protonated and the hydride complexes can be formed in the reaction mixture in comparable amounts. Therefore, the possibility of the second protonation of the hydride complex ***cis*-4d+** (Scheme 4) has been also investigated. The Cl atom

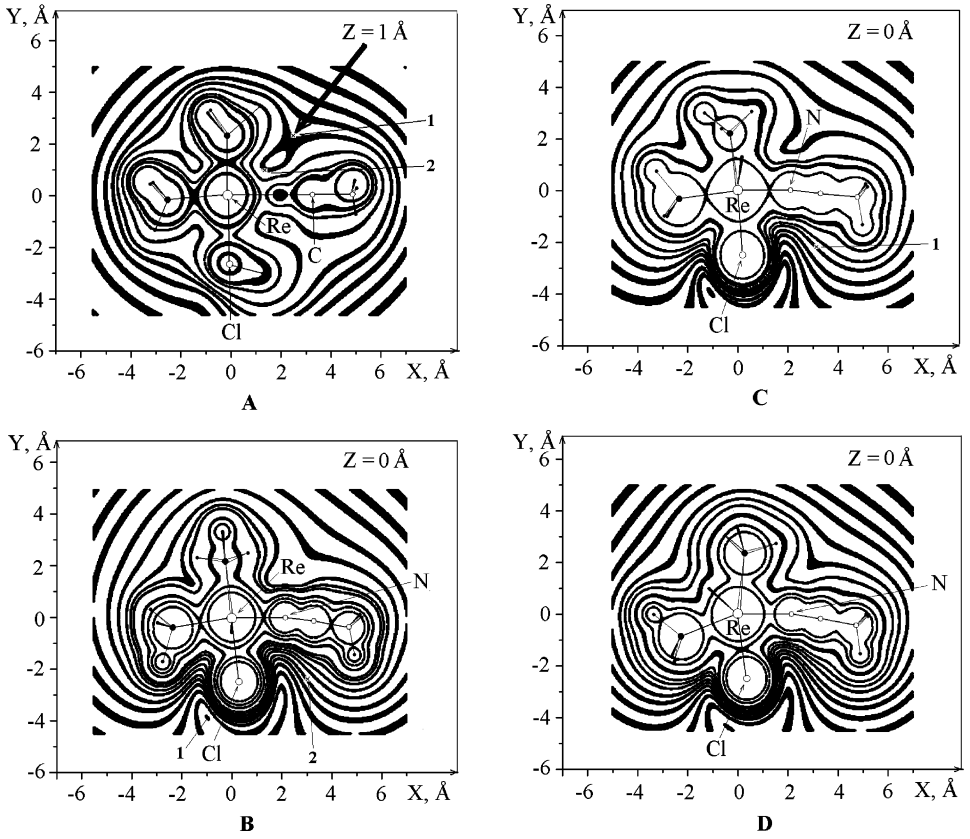

Figure 4. Distribution of positive electrostatic potential for the complexes ***cis*-5a**+ (A), ***cis*-4d**+ (B), ***cis*-4b**+ (C), and ***cis*-4a**+ (D). The points of the initial proton position at the geometry optimization of the diprotonated structures are indicated by Arabic numerals.

again is the most probable site of the electrophilic attack of ***cis*-4d**+ because (i) ESP has the least positive magnitudes near the chlorine atom (Figure 4B), the latter has still a noticeable negative atomic charge and (ii) the p-orbital of Cl gives a significant contribution to the HOMO (along with AOs of the Re and β-C atoms, Figure 3). Placement of the second proton at point 1 (Figure 4B) and the following geometry optimization lead to the formation of the structure ***cis*-7b**++. The complex ***cis*-7b**++ is more stable than ***cis*-7a**++ by 1.50 kcal/mol but less stable than ***cis*-6**++ by 1.07 kcal/mol.

In the next possible step of the reaction, the structure ***cis*-7b**++ may undergo either Re → C or Cl → C proton migration (Scheme 4). The first proceeds via **TS5** and results in the structure ***cis*-6**++ with a following easy deprotonation to give the final product ***cis*-3**+ (route 2). However, the calculated activation barrier is very high for such transformation ($\Delta G_s^{\ddagger} =$ 54.18 kcal/mol), thus excluding this route (route 2).

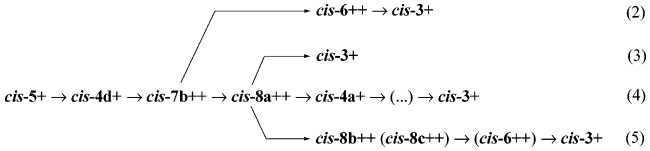

The Cl → C proton-shift occurs through the five-membered cyclic transition state **TS6** to form the hydride-azavinylidene structure ***cis*-8a**++ with an activation barrier of 25.87 kcal/mol, and no direct way for the ***cis*-7b**++ → ***cis*-8b**++ conversion was found.

In the next steps, the complex ***cis*-8a**++ may undergo (i) hydride hydrogen elimination to give the final product ***cis*-3**+ (route 3), (ii) azavinylidene proton elimination with formation of the hydride ***cis*-4a**+ (upon izomerization) (route 4) (the mechanisms based on ***cis*-4a**+ are discussed below), and (iii) migration of the hydride hydrogen within the coordination sphere to give other hydride isomers, first of all ***cis*-8b**++ and ***cis*-8c**++ ([route 5] and see below). For the one-step ***cis*-8a**++ → ***cis*-6**++ process, no transition state was located.

The direct formation of ***cis*-8b**++ from ***cis*-4d**+ upon a second protonation of the latter is also possible although less probable due to electrostatic reasons (see above) and because of the lower stability of ***cis*-8b**++ than that of ***cis*-7b**++. Indeed, as a result of the geometry optimization with the initial position of the second proton at point 2 (Figure 4B), the structure ***cis*-8b**++ was obtained. On the last steps, the easy deprotonation of the complex ***cis*-8b**++ may occur to form ***cis*-3a**+ (route 6). Another possibility to finalize this pathway is the ***cis*-8b**++ → ***cis*-6**++ conversion which takes place via **TS7** with a low activation barrier ($\Delta G_s^{\ddagger} = 6.46$ kcal/mol) (route 7).

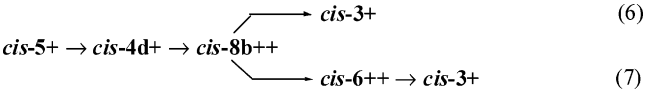

Routes Based on the Hydride and Protonated Chloro *cis*-7a++ Structure. A second group of routes, involving both acid-independent and acid−base-catalyzed pathways, is based on the hydride and protonated chloro species ***cis*-7a**++ (see above, Scheme 4). The latter can undergo (i) a 1,3-H-shift (Re → C) to give ***cis*-6**++ (route 8), (ii) easy deprotonation to form ***cis*-4b**+ (routes 9−10), or (iii) a 1,4-H^+-shift (Cl → C) to yield ***cis*-8c**++ (route 11). For route 8, the transition state **TS8** with the proton position near the N atom (similar to **TS4** for the monoprotonated structures) was located. However, the activation barrier appears to be very high ($\Delta G_s^{\ddagger} = 53.43$ kcal/mol) which rules out the possibility of such a transformation.

The complex ***cis*-4b**+, formed by routes 9 and 10, may undergo a second protonation at either the Cl (reverse reaction)

SCHEME 5: Most Plausible Routes of Protonation of *cis*-[ReCl(NCR)(dppe)$_2$] To Give the Final Azavinylidene Complex[a]

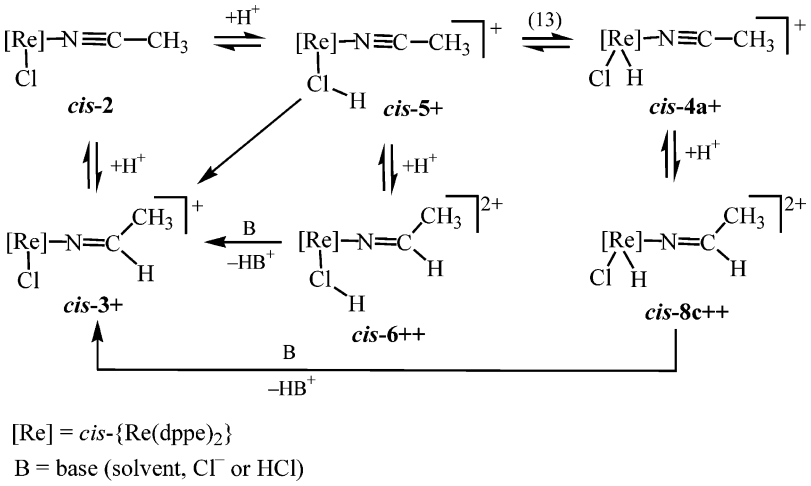

[a] Route 13 is less favorable. The identification of the corresponding models is also indicated.

or the β-C atom (to give ***cis*-8c**++).[70] The ***cis*-4b**+ → ***cis*-8c**++ process is slightly more thermodynamically favored than the ***cis*-4b**+ → ***cis*-7a**++ one ($\Delta\Delta G_s = G_s^{cis-8c++} - G_s^{cis-7a++} = -2.80$ kcal/mol) but the latter is more probable in terms of electrostatic viewpoints (Figure 4C). The route (11) includes the acid-independent ***cis*-7a**++ → ***cis*-8c**++ step leading directly to the Re,C doubly protonated species. This step proceeds via transition state **TS9** with an activation barrier of 23.22 kcal/mol. Finally, the complex ***cis*-8c**++ undergoes deprotonation to give the final species ***cis*-3**+ (routes 10 and 11).

***cis*-5**+ → ***cis*-7a**++ branches to:

***cis*-6**++ → ***cis*-3**+ (8)

***cis*-4b**+ → ***cis*-3**+ (9)

***cis*-4b**+ → ***cis*-8c**++ → ***cis*-3**+ (10)

***cis*-8c**++ → ***cis*-3**+ (11)

Routes Based on the Hydride *cis*-4a+ Structure. The hydride structure ***cis*-4a**+ is the most stable one among the rhenium-protonated species. Hence, the isomerization of the hydrides ***cis*-4d**+ or ***cis*-4b**+ (the complexes involved in the routes discussed above) to ***cis*-4a**+ may take place. The latter complex can also undergo a second protonation at either the Cl or the C atom (routes 12 and 13) (Scheme 4). The first process leads to the structure ***cis*-7c**++, whereas the second one is accompanied by izomerization to give the hydride−azavinylidene complex ***cis*-8c**++. Protonation of the Cl atom is more favorable than that of the C atom (as in the case of ***cis*-4d**+) in terms of electrostatic (Figure 4D), thermodynamic ($\Delta G_s = G_s^{cis-7c++} - G_s^{cis-8c++} = -3.02$ kcal/mol), and FMO (significant contribution of the AO of Cl but not of C in the HOMO, Figure 3) arguments. The extended search of PES shows that the direct Re → C or Cl → C proton shifts are impossible for ***cis*-7c**++, i.e., the formation of the ***cis*-6**++ and ***cis*-8c**++ complexes from ***cis*-7c**++ follows the ***cis*-7c**++ → ***cis*-7a**++ isomerization.

***cis*-5**+ → (...) → ***cis*-4a**+ branches to:

***cis*-7c**++ → ***cis*-7a**++ → (...) → ***cis*-3**+ (12)

***cis*-8c**++ → ***cis*-3**+ (13)

Summarizing the results presented above (sections 2−4), one can conclude the following concerning the mechanism of the ***cis*-5**+ (protonated Cl species) → ***cis*-3**+ (azavinylidene product) conversion. The acid-independent pathway proceeds in one step via 1,4-proton migration from the Cl to the β-C atom (the route ***cis*-5**+ → ***cis*-4d**+ → ***cis*-4b**+ → ***cis*-3**+ via rhenium-protonated structures is not available due to the high activation barrier of the final step). For the acid−base-catalyzed pathway, route 1, i.e., ***cis*-5**+ → ***cis*-6**++ (azavinylidene species with protonated Cl) → ***cis*-3**+, is the most plausible one. Indeed, (i) route 1 includes the formation of only one intermediate ***cis*-6**++, which is easily deprotonated to afford the final complex, which is consistent with the experimental data that show that the acid−base-catalyzed pathway is very fast, and no intermediates were detected due to their short lifetime. (ii) Routes 2−5, 8, 9, and 11 have steps with very high or comparatively higher activation barriers, in contrast with route 1. (iii) For routes 6 and 7, the formation of the doubly protonated complex ***cis*-8b**++ from ***cis*-4d**+ is less favorable thermodynamically by 14.43 kcal/mol than the ***cis*-5a**+ → ***cis*-6**++ reaction. The values of ESP near the β-C atom are slightly less positive for ***cis*-5a**+ than those for ***cis*-4d**+;[71] moreover, route 7 would require the overcome of additional (although low) potential barrier on the ***cis*-8b**++ → ***cis*-6**++ stage. (iv) For routes 8−11, the formation of the ***cis*-7a**++ species is less favorable than that of the ***cis*-6**++ complex in terms of thermodynamic arguments (the former complex is by 2.57 kcal/mol less stable than the latter one) and electrostatic (see Figure 4A and above discussion) and steric factors. (v) Within route 10, the second, comparatively stable intermediate ***cis*-4b**+ (besides the first ***cis*-5a**+ one) should be formed and detected experimentally, which is in contradiction with observations. (vi) The main difficulties of route 12 are connected with the last ***cis*-7a**++ → ***cis*-3**+ transformation (see routes 8−11). (vii) For route 13, although the formation of ***cis*-8c**++ from ***cis*-4a**+ has a probability similar to that for ***cis*-5a**+ → ***cis*-6**++ in route 1 due to close stabilities of the doubly protonated species, the former pathway (as well as the (2)−(7) and (12) ones) requires the overcome of a potential barrier on the ***cis*-5a**+ → ***cis*-4d**+ step, in contrast with route 1; additionally, the deprotonation of the Re atom is sterically hampered for the real system in comparison with H^+ elimination from the Cl ligand, because it would occur under exposure to a base whose molecule should penetrate into the coordination sphere of the metal. Nevertheless, route 13 via hydride intermediates, although less probable than route 1, cannot be completely ruled out as a competitive pathway.

Final Remarks

Extensive theoretical studies of the protonation mechanism of the rhenium nitrile chloro-complexes $[ReCl(NCCH_3)(PH_3)_4]$ (**2**) taken as models for the real species $[ReCl(NCR)(dppe)_2]$ were undertaken at the B3LYP level of theory. The consideration of various factors on the basis of electrostatic arguments, molecular orbital arguments, and thermodynamic, kinetic, and steric features allows one to reach the following main conclusions: (i) The most probable site of the initial proton attack is the chlorine atom that leads to the chloro-protonated intermediates **5**+ with comparatively low stability and high lability of the proton attached. The direct protonation of the nitrile carbon atom to give the final azavinylidene complexes **3**+ is a competitive process, in agreement with the experimental data. (ii) For the cis-isomer of **2** (Scheme 5), the formed intermediate ***cis*-5**+ converts to ***cis*-3**+ by two most plausible pathways: an acid-independent one via 1,4-proton shift and an acid−base catalyzed route involving a second protonation/proton elimination. (iii) A more complicated route including 1,2-H^+-shift from Cl in ***cis*-5**+ to the metal, followed by isomerization of the hydride intermediate to ***cis*-4a**+, a second protonation and elimination of the first proton is also possible (although less probable) as a parallel process.

The theoretical studies also suggest that, in the enzymatic reduction of nitriles, the initial addition can occur to a basic electronegative atom of a neighboring ligand, rather than directly at the substrate itself, forming a more kinetically accessible intermediate which than evolves to a thermodynamically more stable azavinylidene species, upon proton migration from the co-ligand to the nitrile unsaturated carbon. In the active center of the enzyme, the iron−molybdenum cofactor (FeMoCo), such a role, in principle, could be played by a sulfur atom, an oxygen atom of the homocytrate ligand or a nitrogen atom of an imidazole group. In this context, it is noteworthy to mention that the possibility of initial protonation of thiolate ligands at the coordinated sulfur atom has been postulated[72] for some diiron complexes with bridging dinitrogen, proposed as models of nitrogenase.

Acknowledgment. This work has been partially supported by the Fundação para a Ciência e a Tecnologia (FCT) and its POCTI program (FEDER funded) (project QUI/43415/2001) (Portugal). M.L.K. (Grant BPD/16369/98//BPD/5558/2001) is also very much obliged to the FCT and the POCTI program for a fellowship and to Russian Fund for Basic Research for Grant (05-03-32504). The authors thank the computer center of the University of Vienna for technical support and computer time at the Linux-PC clusters Schroedinger II.

Supporting Information Available: Tables of bond lengths, total energies, enthalpies, free Gibbs energies, and Cartesian coordinates of the calculated structures. This material is available free of charge via the Internet at http://pubs.acs.org.

References and Notes

(1) Kukushkin, V. Yu.; Pombeiro, A. J. L. *Chem. Rev.* **2002**, *102*, 1771.

(2) Pombeiro, A. J. L.; Kukushkin, V. Yu. In *Comprehensive Coordination Chemistry II*; McCleverty, J. A., Meyer; T. J., Eds.-in-chief; Elsevier: Amsterdam, 2004; Vol. 1 (Lever; A. B. P., Ed.), Chapter 1.34, p 639.

(3) Kuznetsov, M. L. *Russ. Chem. Rev.* **2002**, *71*, 265.

(4) Pombeiro, A. J. L. *New. J. Chem.* **1994**, *18*, 163.

(5) Michelin, R. A.; Mozzon, M.; Bertani, R. *Coord. Chem. Rev.* **1996**, *147*, 299.

(6) (a) Kukushkin, V. Yu.; Pombeiro, A. J. L. *Inorg. Chim. Acta* **2005**, *358*, 1. (b) Luzyanin, K. V.; Haukka, M.; Bokach, N. A.; Kuznetsov, M. L.; Kukushkin, V. Yu.; Pombeiro, A. J. L. *J. Chem. Soc., Dalton Trans.* **2002**, 1882. (c) Bokach, N. A.; Kukushkin, V. Yu.; Kuznetsov, M. L.; Garnovskii, D. A.; Natile, G.; Pombeiro, A. J. L. *Inorg. Chem.* **2002**, *41*, 2041. (d) Nagao, H.; Hirano, T.; Tsuboya, N.; Shiota, S.; Mukaida, M.; Oi, T.; Yamasaki, M. *Inorg. Chem.* **2002**, *41*, 6267. (e) Michelin, R. A.; Mozzon, M.; Bertani, R.; Benetollo, F.; Bombieri, G.; Angelici, R. J. *Inorg. Chim. Acta* **1994**, *222*, 327.

(7) Makarycheva-Mikhailova, A. V.; Bokach, N. A.; Kukushkin, V. Yu.; Kelly, P. F.; Gilby, L. M.; Kuznetsov, M. L.; Holmes, K. E.; Haukka, M.; Parr, J.; Stonehouse, J. M.; Elsegood, M. R. J.; Pombeiro, A. J. L. *Inorg. Chem.* **2003**, *42*, 301.

(8) (a) Kuznetsov, M. L.; Bokach, N. A.; Kukushkin, V. Yu.; Pakkanen, T.; Wagner, G.; Pombeiro, A. J. L. *J. Chem. Soc., Dalton Trans.* **2000**, 4683. (b) Garnovskii, D. A.; Pombeiro, A. J. L.; Haukka, M.; Sobota, P.; Kukushkin, V. Yu. *Dalton Trans.* **2004**, 1097. (c) Makarycheva-Mikhailova, A. V.; Haukka, M.; Bokach, N. A.; Garnovskii, D. A.; Galanski, M.; Keppler, B. K.; Pombeiro, A. J. L.; Kukushkin, V. Yu. *New J. Chem.* **2002**, *26*, 1085. (d) Kukushkin, V. Yu.; Pakhomova, T. B.; Bokach, N. A.; Wagner, G.; Kuznetsov, M. L.; Galanski, M.; Pombeiro, A. J. L. *Inorg. Chem.* **2000**, *39*, 216.

(9) Wagner, G.; Pombeiro, A. J. L.; Kukushkin, Yu. N.; Pakhomova, T. B.; Ryabov, A. D.; Kukushkin, V. Yu. *Inorg. Chim. Acta* **1999**, *292*, 272.

(10) Luzyanin, K. V.; Kukushkin, V. Yu.; Kuznetsov, M. L.; Garnovskii, D. A.; Haukka, M.; Pombeiro, A. J. L. *Inorg. Chem.* **2002**, *41*, 2981.

(11) (a) Bhandari, S.; Frost, C. G.; Hague, C. E.; Mahon, M. F.; Molloy, K. C. *J. Chem. Soc., Dalton Trans.* **2000**, 663. (b) Bhandari, S.; Mahon, M. F.; Molloy, K. C.; Palmer, J. S.; Sayers, S. F. *J. Chem. Soc., Dalton Trans.* **2000**, 1053. (c) Bhandari, S.; Mahon, M. F.; Molloy, K. C. *J. Chem. Soc., Dalton Trans.* **1999**, 1951. (d) Curran, D. P.; Hadida, S.; Kim, S.-Y. *Tetrahedron* **1999**, *55*, 8997. (e) McMurray, J. S.; Khabashesku, O.; Birtwistle, J. S.; Wang, W. *Tetrahedron Lett.* **2000**, *41*, 6555. (f) Gyoung, Y. S.; Shim, J.-G.; Yamamoto, Y. *Tetrahedron Lett.* **2000**, *41*, 4193. (g) Bethel, P. A.; Hill, M. S.; Mahon, M. F.; Molloy, K. C. *J. Chem. Soc., Perkin Trans. 1* **1999**, 3507.

(12) (a) Kuznetsov, M. L.; Kukushkin, V. Yu.; Dement'ev, A. I.; Pombeiro, A. J. L. *J. Phys. Chem. A* **2003**, *107*, 6108. (b) Wagner, G.; Haukka, M.; Fraústo da Silva, J. J. R.; Pombeiro, A. J. L.; Kukushkin, V. Yu. *Inorg. Chem.* **2001**, *40*, 264. (c) Wagner, G.; Pombeiro, A. J. L.; Kukushkin, V. Yu. *J. Am. Chem. Soc.* **2000**, *122*, 3106. (d) Charmier, M. A. J.; Kukushkin, V. Yu.; Pombeiro, A. J. L. *Dalton Trans.* **2003**, 2540.

(13) (a) Kuznetsov, M. L.; Kukushkin, V. Yu.; Haukka, M.; Pombeiro, A. J. L. *Inorg. Chim. Acta* **2003**, *356*, 85. (b) Bokach, N. A.; Khripoun, A. V.; Kukushkin, V. Yu.; Haukka, M.; Pombeiro, A. J. L. *Inorg. Chem.* **2003**, *42*, 896.

(14) Seino, H.; Mizobe, Y.; Hidai, M. *Chem. Rec.* **2001**, *1*, 349.

(15) Pombeiro, A. J. L.; Hughes, D. L.; Richards, R. L. *J. Chem. Soc., Chem. Commun.* **1988**, 1052.

(16) Amatore, C.; Fraústo da Silva, J. J. R.; Guedes da Silva, M. F. C.; Pombeiro, A. J. L.; Verpeaux, J.-N. *J. Chem. Soc., Chem. Commun.* **1992**, 1289.

(17) Pombeiro, A. J. L. *Inorg. Chim. Acta* **1992**, *200*, 179.

(18) Fraústo da Silva, J. J. R.; Guedes da Silva, M. F. C.; Henderson, R. A.; Pombeiro, A. J. L.; Richards, R. L. *J. Organomet. Chem.* **1993**, *461*, 141.

(19) Guedes da Silva, M. F. C.; Fraústo da Silva, J. J. R.; Pombeiro, A. J. L. *Inorg. Chem.* **2002**, *41*, 219.

(20) Seino, H.; Tanabe, Y.; Ishii, Y.; Hidai, M. *Inorg. Chim. Acta* **1998**, *280*, 163.

(21) Field, L. D.; Jones, N. G.; Turner, P. *Organometallics* **1998**, *17*, 2394.

(22) Tanabe, Y.; Seino, H.; Ishii, Y.; Hidai, M. *J. Am. Chem. Soc.* **2000**, *122*, 1690.

(23) Autissier, V.; Henderson, R. A.; Pickett, C. J. *Chem. Commun.* **2000**, 1999.

(24) Cunha, S. M. P. R.; Guedes da Silva, M. F. C.; Pombeiro, A. J. L. *Inorg. Chem.* **2003**, *42*, 2157.

(25) Hidai, M.; Mizobe, Y. *Chem. Rev.* **1995**, *95*, 1115.

(26) Richards, R. L. *Coord. Chem. Rev.* **1996**, *154*, 83.

(27) Mackay, B. A.; Fryzuk, M. D. *Chem. Rev.* **2004**, *104*, 385.

(28) Pombeiro, A. J. L.; Richards, R. L. *Coord. Chem. Rev.* **1990**, *104*, 13.

(29) Kuznetsov, M. L.; Pombeiro, A. J. L. *Dalton Trans.* **2003**, 738.

(30) (a) Szasz, L. *Pseudopotential Theory of Atoms and Molecules*; Wiley: New York, 1985. (b) Krauss, M.; Stevens, W. J. *Annu. Rev. Phys. Chem.* **1984**, *35*, 357.

(31) Frisch, M. J.; Trucks, G. W.; Schlegel, H. B.; Scuseria, G. E.; Robb, M. A.; Cheeseman, J. R.; Zakrzewski, V. G.; Montgomery, J. A., Jr.; Stratmann, R. E.; Burant, J. C.; Dapprich, S.; Millam, J. M.; Daniels, A. D.; Kudin, K. N.; Strain, M. C.; Farkas, O.; Tomasi, J.; Barone, V.; Cossi, M.; Cammi, R.; Mennucci, B.; Pomelli, C.; Adamo, C.; Clifford, S.; Ochterski, J.; Peterson, G. A.; Ayala, P. Y.; Cui, Q.; Morokuma, K.; Malick, D. K.; Rabuck, A. D.; Raghavachari, K.; Foresman, J. B.; Cioslowski, J.;

Ortiz, J. V.; Baboul, A. G.; Stefanov, B. B.; Liu, G.; Liashenko, A.; Piskorz, P.; Komaromi, I.; Gomperts, R.; Martin, R. L.; Fox, D. J.; Keith, T.; Al-Laham, M. A.; Peng, C. Y.; Nanayakkara, A.; Challacombe, M.; Gill, P. M. W.; Johnson, B.; Chen, W.; Wong, M. W.; Andres, J. L.; Gonzalez, C.; Head-Gordon, M.; Replogle, E. S.; Pople, J. A. *Gaussian 98*, revision A.9; Gaussian, Inc.: Pittsburgh, PA, 1998.

(32) Becke, A. D. *J. Chem. Phys.* **1993**, *98*, 5648.

(33) Lee, C.; Young, W.; Parr, R. G. *Phys. Rev.* **1988**, *B37*, 785.

(34) Andrae, D.; Haeussermann, U.; Dolg, M.; Stoll, H.; Preuss, H. *Theor. Chim. Acta* **1990**, *77*, 123.

(35) (a) Fukui, K. *Acc. Chem. Res.* **1981**, *14*, 363. (b) Gonzalez, C.; Schlegel, H. B. *J. Chem. Phys.* **1991**, *95*, 5853. (c) Gonzalez, C.; Schlegel, H. B. *J. Chem. Phys.* **1989**, *90*, 2154. (d) Gonzalez, C.; Schlegel, H. B. *J. Phys. Chem.* **1990**, *94*, 5523.

(36) Tomasi, J.; Persico, M. *Chem. Rev.* **1997**, *94*, 22027.

(37) Barone, V.; Cossi, M. *J. Phys. Chem.* **1998**, *102*, 1995.

(38) Pearson, R. G. *J. Am. Chem. Soc.* **1983**, *105*, 7512.

(39) Yang, W.; Mortier, M. J. *J. Am. Chem. Soc.* **1986**, *108*, 5708.

(40) Reed, A. E.; Curtiss, L. A.; Weinhold, F. *Chem. Rev.* **1988**, *88*, 899.

(41) Zhang, L.; Guedes da Silva, M. F. C.; Kuznetsov, M. L.; Gamasa, M. P.; Gimeno, J.; Fraústo da Silva, J. J. R.; Pombeiro, A. J. L. *Organometallics* **2001**, *20*, 2782.

(42) (a) Bianchini, R.; Chiappe, C.; Moro, G. L.; Lenoir, D.; Lemmen, P.; Goldberg, N. *Chem.—Eur. J.* **1999**, *5*, 1570. (b) Lenoir, D.; Chiappe, C. *Chem.—Eur. J.* **2003**, *9*, 1036. (c) Ruggiero, G. D.; Williams, I. H. *Chem. Commun.* **2002**, 732. (d) Buchanan, J. G.; Charlton, M. H.; Mahon. M. F.; Robinson, J. J.; Ruggiero, G. D.; Williams, I. H. *J. Phys. Org. Chem.* **2002**, *15*, 642. (e) Nichols, J.; Tralka, T.; Goering, B. K.; Wilcox, C. F.; Ganem, B. *Tetrahedron* **1996**, *52*, 3355. (f) Horasan (Kishali), N.; Kara, Y.; Azizoglu, A.; Balci, M. *Tetrahedron* **2003**, *59*, 3691.

(43) Pissarev, S. A.; Shevchenko, N. E.; Nenaidenko, V. G.; Balenkova, E. S. *Russ. Chem. Bull.* **2003**, *52*, 1667.

(44) (a) Viruela-Martín, P.; Zicovich-Wilson, C. M.; Corma, A. *J. Phys. Chem.* **1993**, *97*, 13713. (b) Thorsteinsson, T.; Famulari, A.; Raimondi, M. *Int. J. Quantum Chem.* **1999**, *74*, 231. (c) Guiling, Z.; Gang, L.; Baiqing, D. *J. Mol. Catal. A* **1999**, *147*, 33.

(45) Esteves, P. M.; Ramírez-Solís, A.; Mota, C. J. A. *J. Phys. Chem. B* **2001**, *105*, 4331.

(46) Ma, N. L.; Wong. M. W. *Eur. J. Org. Chem.* **2000**, 1411.

(47) Lamsabhi, M.; Alcamí, M.; Mó, O.; Bouab, W.; Esseffar, M.; Abboud, J. L.-M.; Yáñez, M. *J. Phys. Chem. A* **2000**, *104*, 5122.

(48) Lee, T. J.; Rice, J. E. *J. Phys. Chem.* **1993**, *97*, 6637.

(49) Mora. M. A.; Galicia, L.; Mora-Ramirez, M. A. *Int. J. Quantum Chem.* **2004**, *97*, 983.

(50) Sroczynski, D.; Grzejdziak, A.; Nazarski, R. B. *J. Incl. Phenom. Macrocyc. Chem.* **1999**, *35*, 251.

(51) Werstiuk, N. H.; Brown, R. S.; Wang, Q. *Can. J. Chem.* **1996**, *74*, 524.

(52) Serrar, C.; Es-sofi, A.; Boutalib, A.; Ouassas, A.; Jarid, A. *J. Mol. Struct. (THEOCHEM)* **1999**, *491*, 161.

(53) Shagun, V. A.; Sinegovskaya, L. M.; Toryashinova, D. S. D.; Mal'kina, A. G.; Brandsma, L.; Trofimov, B. A. *Russ. Chem. Bull.* **2000**, *49*, 1691.

(54) Eckert-Maksic, M.; Glasovac, Z.; Maksic, Z. B.; Zrinski, I. *J. Mol. Struct. (THEOCHEM)* **1996**, *366*, 173.

(55) (a) Szabó, K. J. *Chem.—Eur. J.* **2000**, *6*, 4413. (b) Wallner, O. A.; Szabó, K. J. *Chem.—Eur. J.* **2003**, *9*, 4025.

(56) Bräuer, M.; Weston, J.; Anders, E. *J. Org. Chem.* **2000**, *65*, 1193.

(57) Merlic, C. A.; Miller, M. M.; Hietbrink, B. N.; Houk, K. N. *J. Am. Chem. Soc.* **2001**, *123*, 4904.

(58) Kuznetsov, M. L.; Pombeiro, A. J. L.; Dement'ev, A. I. *J. Chem. Soc., Dalton Trans.* **2000**, 4413.

(59) Tokunaga, M.; Suzuki, T.; Koga, N.; Fukushima, T.; Horiuchi, A.; Wakatsuki, Y. *J. Am. Chem.* Soc. **2001**, *123*, 11917.

(60) Khandogin, J.; Musier-Forsyth, K.; York, D. M. *J. Mol. Biol.* **2003**, *330*, 993.

(61) Kholdeeva, O. A.; Trubitsina, T. A.; Maksimovskaya, R. I.; Golovin, A. V.; Neiwert, W. A.; Kolesov, B. A.; López, X.; Poblet, J. M. *Inorg. Chem.* **2004**, *43*, 2284.

(62) Pombeiro, A. J. L.; Guedes da Silva, M. F. C.; Hughes, D. L.; Richards, R. L. *Polyhedron* **1989**, *8*, 1872.

(63) Fukui, K. *Theory of Orientation and Stereoselection*; Springer-Verlag: Berlin, 1975.

(64) Geerlings, P.; Proft, F. D.; Langenaeker, W. *Chem. Rev.* **2003**, *103*, 1793.

(65) (a) Ponti, A. *J. Phys. Chem. A* **2000**, *104*, 8843. (b) Chandrakumar, K. R. S.; Pal, S. *J. Phys. Chem. A* **2002**, *106*, 5737. (c) Chandrakumar, K. R. S.; Pal, S. *J. Phys. Chem. A* **2002**, *106*, 11775. (d) Chandrakumar, K. R. S.; Pal, S. *J. Phys. Chem. A* **2003**, *107*, 5755. (e) Pal, S.; Chandrakumar, K. R. S. *J. Am. Chem. Soc.* **2000**, *122*, 4145. (f) Deka, R. C.; Ajitha, D.; Hirao, K. *J. Phys. Chem. B* **2003**, *107*, 8574. (g) Romero, M. L.; Méndez, F. *J. Phys. Chem. A* **2003**, *107*, 5874. (h) Mondal, P.; Hazarika, K. K.; Deka, R. C. *Phys. Chem. Commun.* **2003**, *6*, 24. (i) Proft, F. D.; Vivas-Reyes, R.; Biesemans, M.; Willem, R.; Martin, J. M. L.; Geerlings, P. *Eur. J. Inorg. Chem.* **2003**, 3803 and references therein.

(66) Chatterjee, A.; Suzuki, T. M.; Takahashi, Y.; Tanaka, D. A. P. *Chem.—Eur. J.* **2003**, *9*, 3920 and references therein.

(67) For **TS1**, the Cl···H and H···C distances are 1.516 and 1.589 Å, respectively, and the ClHC angle is 143.6°. The analysis of the vectors associated with the "imaginary frequency" and the IRC calculations suggest that **TS1** corresponds to 1,4-H-shift (***cis*-5a**+ → ***cis*-3a**+ conversion). $\Delta E_s^{\ddagger}$ values were calculated as the difference of the total CPCM-energies of **TS1** and ***cis*-5a**+.

(68) The "imaginary frequency" for **TS3** has a rather low value (70.7i cm^{-1}) corresponding to the distortion of the coordination polyhedron.

(69) Here and further, unless stated otherwise, the ΔG_s difference is given for the relative stabilities and activation barriers. See the section "Computational Details" for the estimate of $G_{s.}$

(70) The structure ***cis*-8c**++ is formed at the geometry optimization with the initial H^+ position near ***cis*-4b**+ at point 1, Figure 4C.

(71) ESP values are 0.114 and 0.120 au for ***cis*-5a**+ and ***cis*-4d**+, respectively, at the point at a 3 Å distance above the C atom in the *xy* plane (Figure 4, parts A and B).

(72) Sellmann, D.; Sutter, J. *Acc. Chem. Res.* **1997**, *30*, 460.